IMAGE SUPER-RESOLUTION FROM COMPRESSED SENSING OBSERVATIONS

Wael Saafin[1]*, Miguel Vega*[2]*, Rafael Molina*[1]*, and Aggelos K. Katsaggelos*[3]

[1] Dept. of Computer Science and Artificial Intellegence, University of Granada, Granada, Spain.
[2] Dept. of Languages and Information Systems, University of Granada, Granada, Spain.
[3] Dept. of Electrical Engineering and Computer Science, Northwestern University, Evanston, USA
waelsaafin@hotmail.com, mvega@ugr.es, rms@decsai.ugr.es, aggk@eecs.northwestern.edu

ABSTRACT

In this work we propose a novel framework to obtain High Resolution (HR) images from Compressed Sensing (CS) imaging systems capturing multiple Low Resolution (LR) images of the same scene. The proposed CS Super Resolution (SR) approach combines existing CS reconstruction algorithms with an LR to HR approach based on the use of a Super Gaussian (SG) regularization term. The reconstruction is formulated as a constrained optimization problem which is solved using the Alternate Direction Methods of Multipliers (ADMM). The image estimation subproblem is solved using Majorization-Minimization (MM) while the CS reconstruction becomes an l_1-minimization subject to a quadratic constraint. The performed experiments show that the proposed method compares favorably to classical SR methods at compression ratio 1, obtaining excellent SR reconstructions at ratios below one.

Index Terms— Super resolution, compressed sensing, image sampling, image reconstruction, image enhancement

1. INTRODUCTION

CS theory offers a framework for simultaneous sensing and compression of signals. It establishes that a sparsely representable image/signal can be recovered from a highly incomplete set of measurements [1].

The design of CS image/video cameras (see [2, 3, 4, 5, 6]) has fostered the application of typical image processing tasks to CS observed images. For instance, CS has been applied to areas like radar analysis, face recognition, and biomedical imaging [7]. CS measurements have also been used to recover images observed through unknown blur [8, 9].

Some CS SR problems have also been addressed. For example, coded aperture masks for SR image reconstruction from one image [10], CS imagers acquiring SR images with few sensors [11], and the extension of the single pixel camera concept to a multi-detector device [12] have been proposed. SR from one CS image observation has also been studied [13, 14, 15].

In this paper, SR image reconstruction from multiple CS warped LR observations of the same scene is studied. Since when an HR image is compressive, its warped, blurred, and downsampled versions are also compressive (see [8, 9]), they can be reconstructed from CS observations. Consequently, conventional SR techniques can be applied to estimate an SR image from CS LR observations. In this paper, however, we show that a combined CS SR approach produces better results than first recovering the LR images and then super resolving them. It is important to note here that the proposed framework can be applied to Passive Millimeter Wave (PMMW) images, since the acquired images have very low resolution and CS based PMMW imagers have already been proposed [16, 17].

The rest of this paper is organized as follows. The modeling problem is stated in Section 2. The estimation process is presented in section 3. We demonstrate the effectiveness of the proposed method with experimental results in Section 4 and conclusions are drawn in Section 5.

This paper has been supported by The European Union, Erasmus Mundus program, the Spanish Ministry of Economy and Competitiveness under project TIN2013-43880-R, the European Regional Development Fund (FEDER), the CEI BioTic at the Universidad de Granada, and the Department of Energy (DE-NA0002520).

2. MODELING

In this paper we assume that we have access to a set of Q CS LR observations of the form

$$\mathbf{y}_q = \mathbf{\Phi}\mathbf{z}_q + \mathbf{r}_q \quad q = 1, \ldots, Q, \tag{1}$$

where $\mathbf{y}_q$ is an $M \times 1$ vector representing compressed observations from the LR image $\mathbf{z}_q$, $\mathbf{\Phi}$ is an CS $M \times D$ measurement matrix, $\mathbf{z}_q$ is a column vector of size $D \times 1$ representing the $q-$th LR image and $\mathbf{r}_q$ represents the observation noise. We denote by R the compression ratio of the measurement system, that is R$= M/D$. The sensing matrix $\mathbf{\Phi}$ consists of real entries [18], or it can be binary. The matrix used in our work is of the binary format, since this can be synthesized physically [4, 16, 17]. In both cases the rows/columns of $\mathbf{\Phi}$ are normalized to 1. We assume that the LR observations $\mathbf{z}_q$ are related to an HR image of size N, denoted by the column vector $\mathbf{x}$ by

$$\mathbf{z}_q = \mathbf{A}\mathbf{H}_q\mathbf{C}(\mathbf{s}_q)\mathbf{x} + \mathbf{w}_q = \mathbf{B}_q(\mathbf{s}_q)\mathbf{x} + \mathbf{w}_q, \tag{2}$$

where $\mathbf{A}$ is a $D \times N$ down-sampling matrix, $D \leq N$, where $N = P^2 D$ and P$\geq$1 is the zooming factor, in each direction. $\mathbf{H}_q$ is an assumed known $N \times N$ blurring matrix, $\mathbf{C}(\mathbf{s}_q)$ is the $N \times N$ warping matrix corresponding to the motion vector $\mathbf{s}_q = [\theta_q, d_{hq}, d_{vq}]^t$, where θ_q is the rotation angle, d_{hq} and d_{vq} are respectively the horizontal and vertical translations of the $q-$th LR image with respect to the reference frame, and $\mathbf{w}_q$ is the noise corresponding to the LR acquisition process. Finally, using (1) and (2) we can write

$$\mathbf{y}_q = \mathbf{\Phi}\mathbf{B}_q(\mathbf{s}_q)\mathbf{x} + \mathbf{n}_q\,, \text{ for } q = 1, \ldots, Q, \tag{3}$$

where $\mathbf{n}_q$ represents the combined CS and LR acquisition noise and $\mathbf{x}$ is the HR image we want to estimate. Since $\mathbf{z}_q$ are translated and rotated LR versions of the original image $\mathbf{x}$ (which are assumed to be compressible in a transformed domain). We can estimate the original HR image by recovering first the LR images using CS techniques

then to utilize standard SR techniques on the recovered LR images to obtain the sought HR image. To be precise, if we assume that the LR images are sparse in a transformed domain with $\mathbf{z}_q$=$\mathbf{W}\mathbf{a}_q$, we can recover them from the model in (1) by solving

$$\hat{\mathbf{a}}_q = \arg\min_{\mathbf{a}_q} \frac{\eta}{2} \parallel \mathbf{\Phi W a}_q - \mathbf{y}_q \parallel^2 + \tau \parallel \mathbf{a}_q \parallel_1, \qquad (4)$$

where η, τ are regularization parameters, $\|\,.\,\|$ is the Euclidean norm, and $\|\,.\,\|_1$ the $\ell 1$ norm. Then defining $\hat{\mathbf{z}}_q = \mathbf{W}\hat{\mathbf{a}}_q$ we can estimate the original image by solving

$$\hat{\mathbf{x}} = \arg\min_{\mathbf{x}} \frac{\beta}{2} \sum_q \parallel \mathbf{B}_q(\mathbf{s}_q)\mathbf{x} - \hat{\mathbf{z}}_q \parallel^2 + \alpha\, Q(\mathbf{x}), \qquad (5)$$

where α and β are non-negative parameters, and $Q(\mathbf{x})$ is the following log regularization term

$$Q(\mathbf{x}) = \sum_{d\in\Delta} \sum_{i=1}^{N} \log(|\omega_d^{\mathbf{x}}(i)|)\,, \qquad (6)$$

where $\omega_d^{\mathbf{x}}(i)$ is the i-th pixel of the filtered image

$$\boldsymbol{\omega}_d^{\mathbf{x}} = \mathbf{F}_d\mathbf{x}\,, \qquad (7)$$

where $\mathbf{F}_d$ is a high-pass filter operator, and the index $d \in \Delta$ identifies one of the members of the used filter set. In this paper we have used a filter set with elements $\Delta = \{h, v, hv, vh, hh, vv\}$, where h, v represent the first order horizontal and vertical difference filters, hv and vh represent first order differences along diagonals, and hh and vv the horizontal and vertical second order differences. The regularization term favors sparsity of the high-pass filtered images $\mathbf{F}_d\mathbf{x}$, and corresponds to a Super-Gaussian log prior used in blind deconvolution [19]. We will later explain how to deal with the regularizer at $\boldsymbol{\omega}_d^{\mathbf{x}}(i) = 0$.

As we will show in the experimental section, combining the two sequential optimization problems above into a simultaneous one leads to improved performance, as this enables better exploiting the compressibility of the LR observations using the additional information derived from the estimated HR image. Let $\mathbf{a} = (\mathbf{a}_1, \ldots, \mathbf{a}_q)$ and $\mathbf{s} = (\mathbf{s}_1, \ldots, \mathbf{s}_q)$ and define

$$\begin{aligned} L(\mathbf{x}, \mathbf{a}, \mathbf{s}) = {} & \frac{\eta}{2} \parallel \Phi\mathbf{W}\mathbf{a}_q - \mathbf{y}_q \parallel^2 + \tau \parallel \mathbf{a}_q \parallel_1 \\ & + \frac{\beta}{2} \sum_q \parallel \mathbf{B}_q(\mathbf{s}_q)\mathbf{x} - \mathbf{W}\mathbf{a}_q \parallel^2 + \alpha\, Q(\mathbf{x}), \end{aligned} \qquad (8)$$

Then we can approach the CSSR problem by minimizing $L(\mathbf{x}, \mathbf{a}, \mathbf{s})$ where β is made iteratively large. Alternatively, we can solve

$$\begin{aligned} & \min L(\mathbf{x}, \mathbf{a}, \mathbf{s}) \\ & \text{s.t.} \quad \mathbf{B}_q(\mathbf{s}_q)\mathbf{x} = \mathbf{W}\mathbf{a}_q\,, \text{for } \; q = 1, \ldots, Q\,, \end{aligned} \qquad (9)$$

This is the approach we follow in this paper which will be described in the next section.

3. A SUPER-RESOLUTION FROM COMPRESSED SENSING APPROACH

The constrained optimization problem in (9) is converted into an unconstrained optimization one, and modified to apply ADMM [20, 21]. We define the following augmented Lagrangian functional

$$L(\mathbf{x}, \mathbf{a}, \mathbf{s}, \boldsymbol{\lambda}) = L(\mathbf{x}, \mathbf{a}, \mathbf{s}) + \sum_q \boldsymbol{\lambda}_q^t(\mathbf{B}_q(\mathbf{s}_q)\mathbf{x} - \mathbf{W}\mathbf{a}_q), \qquad (10)$$

where $L(\mathbf{x}, \mathbf{a}, \mathbf{s})$ has been defined in (8) and for $q = 1, \ldots, Q$, $\boldsymbol{\lambda}_q$ are $D \times 1$ Lagrangian multiplier vectors with $\boldsymbol{\lambda} = (\boldsymbol{\lambda}_1, \ldots, \boldsymbol{\lambda}_Q)$. The ADMM gives rise to the following iterative sequence of unconstrained problems,

$$\mathbf{x}^{k+1} = \arg\min_{\mathbf{x}} L(\mathbf{x}, \mathbf{a}^k, \mathbf{s}^k, \boldsymbol{\lambda}^k)\,, \qquad (11)$$

$$\mathbf{a}^{k+1} = \arg\min_{\mathbf{a}} L(\mathbf{x}^{k+1}, \mathbf{a}, \mathbf{s}^k, \boldsymbol{\lambda}^k) \qquad (12)$$

$$\mathbf{s}^{k+1} = \arg\min_{\mathbf{s}} L(\mathbf{x}^{k+1}, \mathbf{a}^{k+1}, \mathbf{s}, \boldsymbol{\lambda}^k) \qquad (13)$$

$$\boldsymbol{\lambda}_q^{k+1} = \boldsymbol{\lambda}_q^k - \beta[\mathbf{B}_q(\mathbf{s}_q^{k+1})\mathbf{x}^{k+1} - \mathbf{W}\mathbf{a}_q^{k+1}] \quad q = 1, \ldots, Q, \qquad (14)$$

where k is the iteration number. Let us now describe how $\mathbf{x}^{k+1}$, $\mathbf{a}^{k+1}$, $\mathbf{s}^{k+1}$, and $\boldsymbol{\lambda}$ are calculated. The calculation of each $\boldsymbol{\lambda}_q^{k+1}$ is straightforward. The function $\rho(s) = \log(|s|+\epsilon)$ in (6) is symmetric around 0, and $\rho(\sqrt{s})$ is concave and increasing for $s \in [0, \infty)$ [19]. So, it can be represented as (see [22])

$$\rho(s) = \inf_{\xi>0} \frac{1}{2}\xi s^2 - \rho^*(\frac{1}{2}\xi)\,, \qquad (15)$$

where $\rho^*(\frac{1}{2}\xi)$ is the concave conjugate function

$$\rho^*(\frac{1}{2}\xi) = \inf_{s>0} \frac{1}{2}\xi s^2 - \rho(s)\,. \qquad (16)$$

It is shown in [19] that the infimum in (15) is achieved when $\xi = \rho'(s)/s$. Consequently, for the regularization term $Q(\mathbf{x})$ in (8), we can write

$$Q(\mathbf{x}) \le R(\mathbf{x}, \boldsymbol{\xi}) = \frac{1}{2} \sum_{d\in\Delta} \mathbf{x}^t\mathbf{F}_d^t\mathbf{\Omega}_d\mathbf{F}_d\mathbf{x} - \sum_{d\in\Delta}\sum_{i=1}^{N} \rho^*(\frac{1}{2}\xi_d(i)) \qquad (17)$$

where $\boldsymbol{\xi} = (\boldsymbol{\xi}_1, \ldots, \boldsymbol{\xi}_Q)$, $\boldsymbol{\xi}_q = (\xi_q(1), \ldots, \xi_q(N))$ for $q = 1, \ldots, Q$, with all its components positive, and $\mathbf{\Omega}_d$ is a diagonal matrix with entries

$$\Omega_d(i, i) = \xi_d(i)\,, \qquad (18)$$

For a given $\mathbf{x}$, the first inequality in (17) becomes an equality if (see [19] for details),

$$\xi_d^{\mathbf{x}}(i) = \frac{1}{|\omega_d^{\mathbf{x}}(i)|^2 + \epsilon}\,, \qquad (19)$$

where $\omega_d^{\mathbf{x}}(i)$ is defined from $\mathbf{x}$ using (7), $\epsilon > 0$ is added to avoid division by zero. Then we can apply standard Majorization-Minimization (MM) methods [23]. Given $\mathbf{x}^k, \mathbf{a}^k, \mathbf{s}^k$ and defining

$$\begin{aligned} L^k(\mathbf{x}) = {} & \frac{\beta}{2} \sum_q \parallel \mathbf{B}_q(\mathbf{s}_q^k)\mathbf{x} - \mathbf{W}\mathbf{a}_q^k \parallel^2 \\ & + \sum_q \boldsymbol{\lambda}_q^{k\,t}(\mathbf{B}_q(\mathbf{s}_q^k)\mathbf{x} - \mathbf{W}\mathbf{a}_q^k) \end{aligned} \qquad (20)$$

we have

$$L^k(\mathbf{x}^k) + \alpha Q(\mathbf{x}^k) = L^k(\mathbf{x}^k) + \alpha R(\mathbf{x}^k, \boldsymbol{\xi}^{\mathbf{x}^k}) \qquad (21)$$

$$\ge L^k(\mathbf{x}^{k+1}) + \alpha R(\mathbf{x}^{k+1}, \boldsymbol{\xi}^{\mathbf{x}^k}) \qquad (22)$$

$$\ge L^k(\mathbf{x}^{k+1}) + \alpha R(\mathbf{x}^{k+1}, \boldsymbol{\xi}^{\mathbf{x}^{k+1}}) \qquad (23)$$

$$= L^k(\mathbf{x}^{k+1}) + \alpha Q(\mathbf{x}^{k+1}) \qquad (24)$$

where

$$\mathbf{x}^{k+1} = \arg\min_{\mathbf{x}} \left\{ \frac{\beta}{2} \sum_q \parallel \mathbf{B}_q(\mathbf{s}_q^k)\mathbf{x} - \mathbf{W}\mathbf{a}_q \parallel^2 + \alpha R(\mathbf{x}, \boldsymbol{\xi}^{\mathbf{x}^k}) + \sum_q \boldsymbol{\lambda}_q^{k\,t}(\mathbf{B}_q(\mathbf{s}_q^k)\mathbf{x} - \mathbf{W}\mathbf{a}_q^k) \right\} \quad (25)$$

Then, the optimization step in (11) produces the following linear equation for $\mathbf{x}^{k+1}$

$$\left[\beta \sum_q \mathbf{B}^{k\,t}_q(\mathbf{s}_q^k)\mathbf{B}_q^k(\mathbf{s}_q^k) + \alpha \sum_{d\in\Delta} \mathbf{F}_d^t \boldsymbol{\Omega}_d^k \mathbf{F}_d \right] \mathbf{x}^{k+1} = \sum_q \mathbf{B}_q^k(\mathbf{s}_q^k)^t \left[\beta \mathbf{W}\mathbf{a}_q^k - \lambda_q^k \right] \quad (26)$$

where

$$\Omega_d^k(i,i) = \frac{1}{\epsilon + |\omega_d^{\mathbf{x}^k}(i)|^2} \quad (27)$$

and $\epsilon > 0$ is included to avoid division by zero.

The optimization step in (12) for each $\mathbf{a}_q$ produces

$$\mathbf{a}_q^{k+1} = \arg\min_{\mathbf{a}_q} \left\{ \frac{\eta}{2} \parallel \boldsymbol{\Phi}\mathbf{W}\mathbf{a}_q - \mathbf{y}_q \parallel^2 + \tau \parallel \mathbf{a}_q \parallel_1 + \frac{\beta}{2} \parallel \mathbf{B}_q^k(\mathbf{s}_q^k)\mathbf{x}^{k+1} - \mathbf{W}\mathbf{a}_q \parallel^2 - \boldsymbol{\lambda}_q^{k\,t}(\mathbf{B}_q^k(\mathbf{s}_q^k)\mathbf{x} - \mathbf{W}\mathbf{a}_q) \right\} \quad (28)$$

which is equivalent to

$$\mathbf{a}_q^{k+1} = \arg\min_{\mathbf{a}_q} \left\{ \frac{\eta}{2} \parallel \boldsymbol{\Phi}\mathbf{W}\mathbf{a}_q - \mathbf{y}_q \parallel^2 + \frac{\beta}{2} \parallel \mathbf{B}_q^k(\mathbf{s}_q^k)\mathbf{x}^{k+1} - \boldsymbol{\lambda}_q^k - \mathbf{W}\mathbf{a}_q \parallel^2 + \tau \parallel \mathbf{a}_q \parallel_1 \right\} \quad (29)$$

The above equation can be rewritten as

$$\mathbf{a}_q^{k+1} = \arg\min_{\mathbf{a}_q} \parallel \boldsymbol{\Phi}'\mathbf{W}\mathbf{a}_q - \mathbf{J}' \parallel^2 + \tau \parallel \mathbf{a}_q \parallel_1 \quad (30)$$

where

$$\mathbf{J}' = \begin{bmatrix} \sqrt{\frac{\eta}{2}}\mathbf{y}_q \\ \sqrt{\frac{\beta}{2}}(\mathbf{B}_q^k(\mathbf{s}_q^k)\mathbf{x}^{k+1} - \boldsymbol{\lambda}_q^k) \end{bmatrix} \text{ and } \boldsymbol{\Phi}' = \begin{bmatrix} \sqrt{\frac{\eta}{2}}\boldsymbol{\Phi} \\ \sqrt{\frac{\beta}{2}}\mathbf{I} \end{bmatrix} \quad (31)$$

with $\mathbf{I}$ the $D \times D$ identity matrix.

The above optimization problem can be solved using the algorithm in [24].

To update the registration parameters, we need to solve

$$\mathbf{s}_q^{k+1} = \arg\min_{\mathbf{s}_q} \parallel \mathbf{B}_q(\mathbf{s}_q)\mathbf{x}^{k+1} - \mathbf{W}\mathbf{a}_q^{k+1} \parallel^2 \quad (32)$$

However we have experimentally observed that a fast and reliable estimation of the registration parameters can be obtained by estimating the warping parameters between the reconstructed LR observations with respect to the reference observation, rather than the estimated HR image. Thus minimising

$$\mathbf{s}_q^{k+1} = \arg\min_{\mathbf{s}_q} \parallel \mathbf{C}(\mathbf{s}_q)\mathbf{H}_r^t\mathbf{A}^t\mathbf{W}\mathbf{a}_r^{k+1} - \mathbf{H}_q^t\mathbf{A}^t\mathbf{W}\mathbf{a}_q^{k+1} \parallel^2 \quad (33)$$

where r denotes the reference image assumed to be the first reconstructed LR observation. The complete CSR algorithm is presented in Algorithm 1

Algorithm 1 Compressive Sensing Super Resolution (CSR)

Require: Values α, β, τ, η.
Initialize $\mathbf{a}^0$, $\mathbf{s}^0$, $\boldsymbol{\lambda}^0$, $\boldsymbol{\Omega}^0 = \{\boldsymbol{\Omega}_d^0, d \in \Delta\}$,
$k = 0$
while convergence criterion is not met **do**
1. Calculate $\mathbf{x}^{k+1}$ by solving (26)
2. For $d \in \Delta$, calculate $\boldsymbol{\Omega}_d^{k+1}$ using (27)
3. For $q = 1, \ldots, Q$, calculate $\mathbf{a}_q^{k+1}$ using (30)
4. For $q = 1, \ldots, Q$, calculate $\mathbf{s}_q^{k+1}$ using (33)
5. For $q = 1, \ldots, Q$, update $\boldsymbol{\lambda}_q^{k+1}$ using (14)
6. Set $k = k + 1$
end while
return $\mathbf{x}$

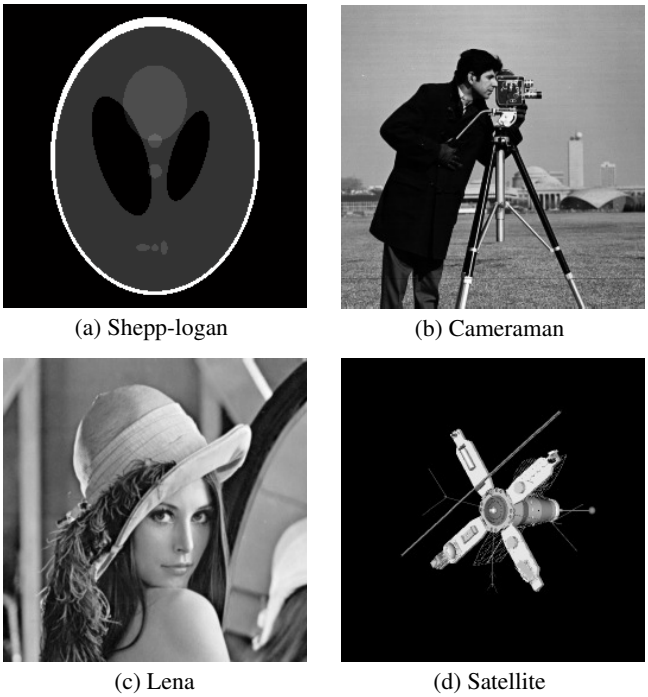

(a) Shepp-logan (b) Cameraman

(c) Lena (d) Satellite

Fig. 1. Original Images

4. EXPERIMENTAL RESULTS

To analyze the behavior of the proposed CSR method we carried out a set of experiments on the images shown in Figure 1, namely the shepp-logan, cameraman, lena, and satellite images. The image is warped using random displacement vectors to account for horizontal, vertical and rotational displacement. Then each image is degraded by a Gaussian blur of different but known variance and it is downsampled. The observation is compressed using a circulant Toeplitz matrix, to serve as a measurement matrix, following the Bernoulli probability distribution. White Gaussian noise, with SNR=40dB, is added to the compressed observations. Figure 2 shows an example of the degradation process. We used a 3-level Haar wavelet transform as a transform basis W, and Peak Signal to Noise Ratio (PSNR) as a performance measure. Three noisy observations were generated for each experiment, and the obtained average PSNR is showed. Stopping criteria are met either when the maximum number of iterations, being eighty, is reached, or when $\frac{norm(\mathbf{x}^k - \mathbf{x}^{k-1})}{norm(\mathbf{x}^{k-1})} \leq 10^{-4}$.

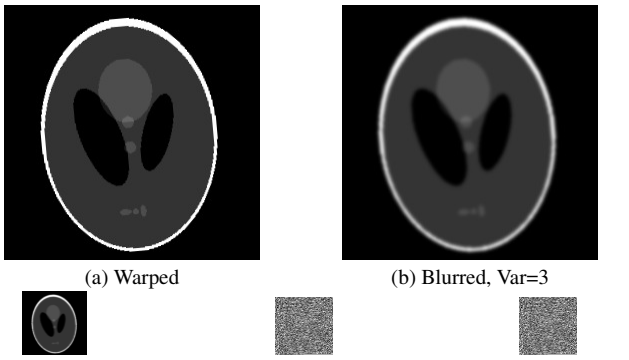

(a) Warped (b) Blurred, Var=3

(c) Down-sampled, P=4 (d) Compressed, R=0.8 (e) Noised, SNR=40dB

Fig. 2. Stages of degradation process.

In the first experiment, we compare our method with the following existing SR methods: Bicubic Interpolation, SR using total variation prior [25], SR using l_1-norm prior [26], SR using simultaneous auto regressive regularization prior [27], Robust SR [28], and Zomet SR [29], all using the default parameters in [30]. The abbreviations we use to refer to them are respectively: Bi, Sv, Sl, Sr, Rt, and Zt. CSR refers to our proposed algorithm, where we used compression ratio R$=1.0$ to comply with the above mentioned algorithms which do not use compressed observations. Results are tabulated in Table 1.

Table 1. Performance comparison for SR algorithms with proposed CSR algorithm, with P=4, SNR=40dB, Q=4 and for CSR R=1.0. Every experiment was repeated three times and the shown values are the average values. In bold are the highest PSNR values.

Img	Alg / Var	Bi	Sv	Sl	Sr	Rt	Zt	CSR
		PSNR Values						
Shp.	3	17.9	21.6	20.7	21.4	20.8	18.7	**26.4**
	5	17.9	21.7	21.2	22.0	20.5	18.7	**25.9**
	7	17.9	21.5	21.6	22.4	20.9	18.8	**25.1**
Cam.	3	20.5	21.8	21.9	22.2	21.1	20.5	**25.2**
	5	20.5	21.8	21.7	22.1	20.9	20.4	**25.0**
	7	20.5	21.7	21.5	21.8	20.7	20.4	**24.3**
Len.	3	21.0	26.0	25.8	26.4	22.2	21.7	**29.1**
	5	21.1	26.3	25.9	26.9	20.1	21.7	**28.2**
	7	21.1	26.0	25.6	26.8	23.4	21.7	**27.5**
Sat.	3	20.5	23.4	21.9	24.1	23.4	21.1	**28.9**
	5	20.6	23.6	20.6	24.2	22.6	21.0	**28.5**
	7	20.6	23.7	21.3	24.2	23.2	21.1	**27.9**

Figure 3 shows a comparison between SR algorithms and the proposed CSR algorithm. Curves of PSNR vs variance of the blur affecting the Shepp-logan image, are shown for R=1.0, for all algorithms.

We now investigate the performance of the proposed CSR algorithm for compression ratios R less than one. For all images we used Gaussian blur of variance 3, zooming factor P=1, and SNR=40dB. The results are shown in Figure 4 for the four images used in our study and different values of R.

Figure 5 shows estimates for $\mathbf{x}$, using CSR, with Blur Var=3, SNR=40dB, Q=5: In 5(a) R=1.0, P=4 while in 5(b) R=0.8, P=4. This figure shows that a 256×256 HR image can be recovered by R=0.8 CS sampling of five 64×64 LR images; with a percentage of 5% of the original image size, and still CSR algorithm is capable of successful reconstruction.

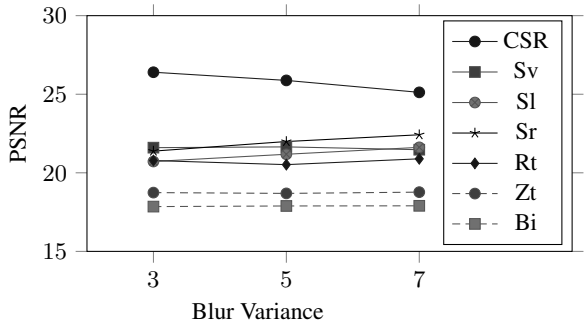

Fig. 3. Comparison between SR algorithms and CSR algorithm for the Shepp-logan image, for P=4, SNR=40dB, Q=4, and for CSR, R=1.0.

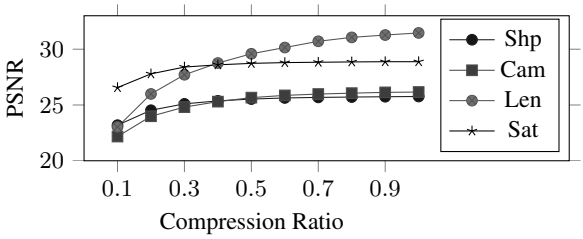

Fig. 4. Performance Measure of proposed CSR vs R. P=1, Blur Var=3, SNR=40dB, Q=3.

(a) R=1.0, P=4 (b) R=0.8 , P=4

Fig. 5. Estimated 256×256 Images using CSR. Q=5, Blur Var=3, SNR=40dB.

5. CONCLUSIONS

In this work we have proposed a framework to recover SR images from multiple CS downsampled and warped observations of the same scene. Any classical SR technique can be incorporated in the developed methodology. At compression ratio one, the proposed approach shows better performance than algorithms dealing with SR without CS. For ratios below one, it also produces high quality reconstructed images. The proposed framework can be extended to compressive video for the estimation of both intra-frame and inter-frame SR. It can also be applied to passive millimeter wave images since those images are inherently LR and CS systems have already been proposed.

6. REFERENCES

[1] EJ Candes and J Romberg, "Practical signal recovery from random projections.," *Wavelet Applications in Signal and Image Processing XI, Proc. SPIE Conf.*, vol. 5914, 2005.

[2] M.F. Duarte, M.A. Davenport, D. Takhar, J.N. Laska, Ting Sun, K.F. Kelly, and R.G. Baraniuk, "Single-pixel imaging via compressive sampling," *Signal Processing Magazine, IEEE*, vol. 25, no. 2, pp. 83–91, March 2008.

[3] W. L. Chan, K. Charan, D. Takhar, K. F. Kelly, R.G. Baraniuk, and D.M. Mittleman, "A single-pixel terahertz imaging system based on compressed sensing," *Applied Physics Letters*, vol. 93, no. 12, pp. 121105–121105–3, Sep 2008.

[4] A. Heidari and D. Saeedkia, "A 2d camera design with a single-pixel detector," in *Infrared, Millimeter, and Terahertz Waves, 2009. IRMMW-THz 2009. 34th International Conference on*, Sept 2009, pp. 1–2.

[5] T. Li, X. Wang, W. Wang, and A. K. Katsaggelos, "Compressive video sensing with limited measurements," *Journal of Electronic Imaging*, vol. 22, no. 4, pp. 043003–043003, 2013.

[6] A.C. Sankaranarayanan, C. Studer, and R.G. Baraniuk, "Cs-muvi: Video compressive sensing for spatial-multiplexing cameras," in *Computational Photography (ICCP), 2012 IEEE International Conference on*, April 2012, pp. 1–10.

[7] Y. C. Eldar and G. Kutyniok, *Compressed sensing: theory and applications*, Cambridge University Press, 2012.

[8] L. Spinoulas, B. Amizic, M. Vega, R. Molina, and A.K. Katsaggelos, "Simultaneous bayesian compressive sensing and blind deconvolution," in *Signal Processing Conference (EUSIPCO), 2012 Proceedings of the 20th European*, Aug 2012, pp. 1414–1418.

[9] B. Amizic, L. Spinoulas, R. Molina, and A.K. Katsaggelos, "Compressive blind image deconvolution," *Image Processing, IEEE Transactions on*, vol. 22, no. 10, pp. 3994–4006, Oct 2013.

[10] R. F Marcia and R. M Willett, "Compressive coded aperture superresolution image reconstruction," in *Acoustics, Speech and Signal Processing, 2008. ICASSP 2008. IEEE International Conference on*. IEEE, 2008, pp. 833–836.

[11] Q. Wang and G. Shi, "Super-resolution imager via compressive sensing," in *Signal Processing (ICSP), 2010 IEEE 10th International Conference on*, Oct 2010, pp. 956–959.

[12] T. Edeler, K. Ohliger, S. Hussmann, and A. Mertins, "Multi image super resolution using compressed sensing," in *Acoustics, Speech and Signal Processing (ICASSP), 2011 IEEE International Conference on*, May 2011, pp. 2868–2871.

[13] A. Fannjiang and W. Liao, "Super-resolution by compressive sensing algorithms," *CoRR*, vol. abs/1211.5870, 2012.

[14] H.P. Babcock, J.R. Moffitt, Y. Cao, and X. Zhuang, "Fast compressed sensing analysis for superresolution imaging using l1-homotopy," *Optics Express*, vol. 21, no. 23, pp. 28583–28596, 2013.

[15] J. Fang, J. Li, Y. Shen, H. Li, and S. Li, "Super-resolution compressed sensing: An iterative reweighted algorithm for joint parameter learning and sparse signal recovery," *Signal Processing Letters, IEEE*, vol. 21, no. 6, pp. 761–765, June 2014.

[16] N. Gopalsami, S. Liao, T. W Elmer, E. R Koehl, A. Heifetz, A. C Raptis, L. Spinoulas, and A. K Katsaggelos, "Passive millimeter-wave imaging with compressive sensing," *OPTICAL ENGINEERING*, vol. 51, no. 9, SEP 2012.

[17] N Gopalsami, TW Elmer, Shaolin Liao, R Ahern, A Heifetz, AC Raptis, M Luessi, D Babacan, and AK Katsaggelos, "Compressive sampling in passive millimeter-wave imaging," in *SPIE Defense, Security, and Sensing*. International Society for Optics and Photonics, 2011, pp. 80220I–80220I.

[18] J. Rubio, M. Vega, R. Molina, and A.K. Katsaggelos, "A general sparse image prior combination in compressed sensing," in *Signal Processing Conference (EUSIPCO), 2013 Proceedings of the 21st European*, Sept 2013, pp. 1–5.

[19] S Derin Babacan, Rafael Molina, Minh N Do, and Aggelos K Katsaggelos, "Bayesian blind deconvolution with general sparse image priors," in *Computer Vision–ECCV 2012*, pp. 341–355. Springer, 2012.

[20] Stephen Boyd, Neal Parikh, Eric Chu, Borja Peleato, and Jonathan Eckstein, "Distributed optimization and statistical learning via the alternating direction method of multipliers," *Foundations and Trends® in Machine Learning*, vol. 3, no. 1, pp. 1–122, 2011.

[21] Y.-H. Xiao and Z.-F. Jin, "An alternating direction method for linear-constrained matrix nuclear norm minimization," *Numerical Linear Algebra with Applications*, vol. 19, no. 3, pp. 541–554, 2012.

[22] R Tyrrell Rockafellar, *Convex analysis*, Number 28. Princeton university press, 1997.

[23] K. Lange, *Optimization*, Springer-Verlag, 2013.

[24] K. Koh, S. J Kim, and S. P Boyd, "An interior-point method for large-scale l1-regularized logistic regression.," *Journal of Machine learning research*, vol. 8, no. 8, pp. 1519–1555, 2007.

[25] S.D. Babacan, R. Molina, and A.K. Katsaggelos, "Variational bayesian super resolution," *IEEE Transactions on Image Processing*, vol. 20, no. 4, pp. 984–999, 2011.

[26] S. Villena, M. Vega, R. Molina, and A.K. Katsaggelos, "Bayesian super-resolution image reconstruction using an l1 prior," in *Image and Signal Processing and Analysis, 2009. ISPA 2009. Proceedings of 6th International Symposium on*, Sept 2009, pp. 152–157.

[27] R. Molina, J. Nez, F.J. Cortijo, and J. Mateos, "Image restoration in astronomy: A bayesian perspective," *IEEE Signal Processing Magazine*, vol. 18, no. 2, pp. 11–29, 2001.

[28] S. Farsiu, M.D. Robinson, M. Elad, and P. Milanfar, "Fast and robust multiframe super resolution," *IEEE Transactions on Image Processing*, vol. 13, no. 10, pp. 1327–1344, 2004.

[29] A. Zomet, A. Rav-Acha, and S. Peleg, "Robust super-resolution," in *Computer Vision and Pattern Recognition, 2001. CVPR 2001. Proceedings of the 2001 IEEE Computer Society Conference on*, 2001, vol. 1, pp. I–645–I–650 vol.1.

[30] S. Villena, M. Vega, S.D. Babacan, R. Molina, and A.K. Katsaggelos, "Bayesian combination of sparse and non-sparse priors in image super resolution," *Digital Signal Processing*, vol. 23, no. 2, pp. 530–541, 2013.